THE JOURNAL OF PHYSICAL CHEMISTRY B

ARTICLE

pubs.acs.org/JPCB

Predictive Model for Diffusion-Limited Aggregation Kinetics of Nanocolloids under High Concentration

Marco Lattuada*

Institute for Chemical- and Bioengineering, Wolfgang-Pauli-Strasse 10, CH-8093 Zurich, Switzerland

ABSTRACT: Smoluchowski's equation for the rate of aggregation of colloidal particles under diffusion-limited conditions has set the basis for the interpretation of kinetics of aggregation phenomena. Nevertheless, its use is limited to sufficiently dilute conditions. In this work we propose a correction to Smoluchowski's equation by using a result derived by Richards (J. Phys. Chem. 1986, 85, 3520) within the framework of trapping theory. This corrected aggregation kernel, which accounts for concentration dependence effects, has been implemented in a population-balance equations scheme and used to model the aggregation kinetics of colloidal particles undergoing diffusion-limited aggregation under concentrated conditions (up to a particle volume fraction of 30%). The predictions of population balance calculations have been validated by means of Brownian dynamic simulations. It was found that the corrected kernel can very well reproduce the results from Brownian dynamic simulations for all concentration values investigated, and is also able to accurately predict the time required by a suspension to reach the gel point. On the other hand, classical Smoluchowski's theory substantially underpredicts the rate of aggregation as well as the onset of gelation, with deviations becoming progressively more severe as the particle volume fraction increases.

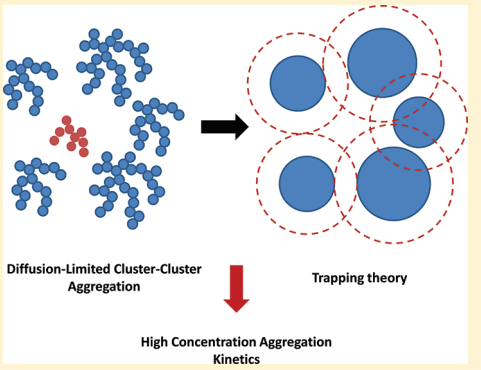

INTRODUCTION

The self-assembly of colloidal (nano)particles has been the subject of a large body of research conducted primarily by the communities of physicists, material scientists and colloidal chemists over the last few decades.[1−3] The importance of this topic is both fundamental and applied. Colloids have been often used as model systems to shed light on phase transition phenomena,[3] and have been considered by physicists as large scale equivalent of atoms, having much slower dynamics, which makes their observation simpler, and with interaction potentials that can be tuned both in magnitude and in range.[1] This makes them ideal candidates to explore new theories and gain better understanding on poorly understood phenomena such as glass transitions and formation of nonequilibrium structures. At the same time, assembly of colloidal particles is very relevant to the processing of many particulate-based materials, such as paints, ceramics, food, and pharmaceutical products, and is very relevant in wastewater treatment.[2,3]

In the world of nanocolloids, aqueous suspensions play a particularly important role. Not only for applications is water the cheapest and environmentally most benign solvent but also its very high dielectric constant allows one to take advantage of electrostatic stabilization of particles.[3] This justifies why aggregation of electrostatically stabilized particles has been one of the most investigated assembly processes.[4−12] Under quiescent conditions, and in the absence of other external forces, the universality underlying this phenomenon has been recognized more than two decades ago by the Weitz group.[5−7] Using a combination of ad hoc experiments and Monte Carlo simulations, Weitz and co-workers pointed out for the first time that the behavior of colloids under either diffusion-limited or reaction-limited conditions is independent of the colloidal particles type and material. The use of Monte Carlo, Brownian dynamics, and other simulations techniques has since then become a common tool to unravel the physics underlying particles self-assembly processes.[8,9,13−15]

Monte Carlo simulations are not the only tool used by theoreticians to investigate aggregation. Many works have also used mean-field kinetic equations, also known as population balance equations, to model the kinetics of aggregation and extract scaling information about the cluster mass distribution.[16] Population balance equations (PBEs) are mass balances on all the clusters formed as a result of an aggregation process, and aggregation events are modeled as second order kinetic processes. In order to make quantitative predictions, the equations require the rate constants of all aggregation events, commonly referred to as kernels. These kernels condense all the physics behind the mechanism driving aggregation. The case of diffusion-limited aggregation has been one of the better understood, and most commonly investigated.[16,17] Smoluchowski formulated the first diffusion-limited kernel almost one century ago, and obtained an exact solution of all kinetic equations under the assumption that the kernel is the same for all the clusters.[18] The accuracy of Smoluchowski's predictions has been the subject of numerous experimental investigations.[1,19,20]

Received: October 11, 2011
Revised: December 4, 2011
Published: December 10, 2011

Population balance equations have attracted the interest not only of physicists, but also of engineers, because of the intrinsic simplicity of the kinetic description.[4,16] However, this approach suffers from a severe limitation: its predictions are usually accurate only under dilute conditions, where simultaneous collisions among more than three particles of clusters are highly unlikely, and many body effects can be neglected.[16] Under concentrated conditions, no accurate predictions can be made by means of the kinetic approach, even though in many relevant industrial processes highly concentrated conditions are of great interest. Additionally, experimental work on aggregation kinetics of fully destabilized colloidal suspensions under concentrated conditions is extremely difficult, because of the very fast dynamics involved, and only relatively low volume fractions can be probed.[21] Even theoretically, only a handful of investigations in the literature have tried to investigate in a quantitative manner the effect of high concentrations on the aggregation kinetics of colloidal nanoparticles.[8,22−25] Sciortino and Tartaglia[26,27] have proposed an elegant model to explain the time evolution of scattering structure factors observed by Carpineti and Giglio[28] for polystyrene particles undergoing DLCA. The model consists of a combination of Smoluchowski's diffusion equation with a mass balance assuming a monodisperse distribution of clusters. The agreement of the model with experimental data and Brownian dynamic simulations are extraordinary, but only for moderately low particle volume fractions (up to 1−2%). A couple of very interesting works recently published by the Pratsinis group have for example shown that both under diffusion-limited conditions and in free-molecular regime high concentrations lead to substantial increase of the aggregation rate as compared to Smoluchowski's equation predictions, up to 30 times for a particle volume fraction of 35%.[22,23] In these works and in a few others some semiempirical corrections to Smoluchowski's equation have been proposed to account for high concentration effects.[24,25,29]

Smoluchowski's equation has been not only used as a milestone in the theory of coagulation kinetics, but at the same time has set the bases for investigating a broad range of diffusion-limited phenomena, such as diffusion-limited chemical reactions of species with a negligible size toward finite-size reactive traps.[30] In this field, instead, a considerable number of studies have been published, with aim of extending Smoluchowski's law to high concentration of traps.[31−46] The studies by Richards and by Torquato's group have greatly contributed to the understanding of these phenomena.[35−41] A common result is that the rate of diffusion-limited reaction is greatly increased by a high concentration of traps, even by more than 50 times, as compared to Smoluchowski's theory predictions.[41] These results have been obtained by using of Monte Carlo simulations, which helped the development of systematic corrections that extend Smoluchowski's theory to higher concentrations.[38]

In this work, we bridge the gap between what has been proposed so far in the field of trapping theory and the case of diffusion-limited aggregation kinetics. A correction for the diffusion-limited aggregation kernel valid at high concentrations has been introduced based on extended version of the equation proposed by Richards for fully penetrable traps.[37] The correction is implemented in a population-balance equation code, and the predictions are compared to the data obtained from Brownian dynamic simulations performed under diffusion-limited aggregation conditions. This new kernel allows one to make accurate predictions of the time evolution of the entire cluster mass distribution, provided that the structural parameters of the clusters (i.e., their fractal dimension) are know. Additionally, the gel point has been estimated with good precision.

BROWNIAN DYNAMIC SIMULATIONS

Nonequilibrium Brownian dynamics (BD) simulations have been performed by implementing a rigid body version of the Langevin dynamics.[24,47−49] Namely, a virtual simulation box is generated and particles are initially randomly positioned inside the box. Periodic boundary conditions are applied to the simulation box, to mimic an infinite size system. The size of the simulation box is adjusted in order to have always about 15000 particles, for all volume fraction values considered in this work. Before starting the real simulation, a series of equilibration steps have been performed, assuming that particles interact only via a short-range electrostatic repulsive potential, with a characteristic length equal to 10% of the particle radius. The equilibrium steps are continued until the total repulsive energy of the system reaches approximately a constant value. The initial time step used during the equilibration steps has been chosen as a fraction of the Brownian time $t_b = R_p^2/D_{iff}$, defined as the time required for a particle with radius R_p and diffusion coefficient D_{iff} to diffuse over a distance of one radius. This fraction has been computed so that in one time step a particle could not move over a distance larger than 5% of the average interparticle surface-to-surface spacing d at that given particle volume fraction ϕ_p, semiempirically estimated as follows:

$$d = 2R_p\left(\left(\frac{0.64}{\phi_p}\right)^{1/3} - 1\right) \quad (1)$$

If during a time step an overlapping between two particles occurs, the time step is reduced to eliminate the overlap.

Once the equilibration has been completed, the real nonequilibrium simulation is initiated. In this case, particle and clusters interact though attractive van der Waals interactions. The fundamental assumption underlying these nonequilibrium simulations is that when two particles or clusters touch, they form a permanent bond, and from that point on a new cluster is formed with a mass equal to the sum of the masses of the two original colliding clusters. This is an assumption commonly utilized in Monte Carlo simulations of diffusion-limited cluster aggregation (DLCA), but has been not been very frequently used in Brownian dynamics.

On of the difficulties related to this approach is that the motion of rigid clusters has to be properly described within the framework of Brownian dynamics. Among the different alternative approaches presented in the literature, including the use do algorithms imposing rigid constraints among its particles,[24] in this work rigid body motion of clusters has been implemented.[50] Inertia of all clusters has been neglected, so that their motion, both translational and rotational, can be described by the overdamped Langevin equation[47]

$$F_{v,i} + F_{V\,dW,i} + F_{B,i} = 0 \quad (2)$$

where $F_{v,i}$ is the viscous force-torque vector, $F_{B,i}$ the Brownian force-torque vector and $F_{VdW,i}$ the total van der Waals force-torque acting on the ith cluster. All these vectors contain six components: three for the force, and three for the torque. The simulations neglect all intercluster hydrodynamic interactions. The total van der Waals force acting on a cluster is computed using pairwise additivity assumption, i.e., adding all interactions

experienced by all particles belonging to the cluster. van der Waals forces between two particles, i and j, located at a dimensionless distance x were computed using Hamaker's expression:[1]

$$U_{V\ dW,ij} = -\frac{A}{6}\left(\frac{2}{x^2-4} + \frac{2}{x^2} + \log\left(\frac{x^2-4}{x^2}\right)\right) \quad (3)$$

with A being the Hamaker constant, $U_{VdW,ij}$ van der Waals interaction energy, and remembering that the force is related to the energy by $F_{VdW,ij} = -\nabla U_{VdW,ij}$, where ∇ is the gradient operator.

Since a cluster has usually a complex structure, its diffusion and hydrodynamic properties are tensorial quantities. This means that the cluster equations of motion are written as follows:[1,50]

$$V_i = \frac{\mathbf{D}_{iff,i}}{kT} F_{V\ dW,i} + V_{B,i} = 0 \quad (4)$$

Here V_i is the velocity vector, $\mathbf{D}_{iff,i}$ the diffusion tensor and $V_{B,i}$ the Brownian contribution to the velocity of the ith cluster. All the velocity vectors have six components and include both translation and rotational velocities. The Brownian contribution to the velocity has the following property[1]

$$\langle V_{B,i}(t) V_{B,i}(t')\rangle = 2\mathbf{D}_{iff,i}\delta(t-t') \quad (5)$$

where $\delta(t - t')$ is Dirac delta function. The corresponding equation for the displacement is the following:[1]

$$\Delta X_i = \frac{\mathbf{D}_{iff,i}}{kT} F_{V\ dW,i}\, dt + \mathbf{M}_i\sqrt{2\ dt} = 0 \quad (6)$$

$\mathbf{M}_i\mathbf{M}_i = \mathbf{D}_{iff,i}$ and ΔX_i is the displacement vector of the ith cluster, containing both translational and angular increments. For implementation purpose, quaternions are used to keep track of the orientation of a cluster.[47]

In order to perform all these calculations, the mobility tensor of a cluster has to be computed. This is performed whenever a new cluster is formed. The diffusion tensor is computed using the theory proposed by Garcia de la Torre et al.[51,52] This approach, based on the Kirkwood−Rieseman theory, allows one to account for hydrodynamic interactions inside a cluster and thus is able to account for both the fractal scaling of clusters diffusion coefficients and for the anisotropy in their diffusion tensor. However, since the computation of the diffusion tensor of a cluster with N particles requires the inversion of a $3N \times 3N$ matrix, the procedure is only applied to clusters with less than 500 particles. For larger clusters, a more simplified assumption is used, as reported by Garcia de la Torre's group.[53] According to this second approach, called double summation approach, the rotational diffusion tensor is isotropic, and only the translational part of the diffusion tensor maintains an anisotropic form.

The equations of motion (eq 6) are integrated using a predictor-corrector algorithm. The collision between two clusters is handled as follows. If during a time step there is an overlap between two particles, the time step is reduced iteratively, until the exact step size is obtained that reduces the interparticle distance to one particle diameter, so that a new bond can be formed. Every time that the total number of clusters has decreased by 10%, the entire cluster mass distribution is stored in a file. Each simulation continues until only one percolating cluster remains in the system, representing the gel phase. In order to achieve a good statistics, at least 10 simulations for each investigated volume fraction have been performed, and the range of particle volume fractions analyzed was $0.01 \le \phi_p \le 0.3$.

HIGH CONCENTRATION KERNEL CORRECTION

In order to account for the effect of high concentration on the kinetics of aggregation, we borrowed concepts from the well developed trapping theory, and in particular from the works by Torquato and co-workers and by Richards.[35−41,54]

Trapping theory has focused on studying diffusion of small reactant molecules in heterogeneous media, in which the disperse phase behaves as a collection of immobile traps. Under diffusion-limited conditions, traps behave as objects that instantly absorb any molecule that collides with them. One of the objective of trapping theories is to compute the rate of diffusion limited reactions in a system containing a given concentration of traps. As model traps, usually spheres are considered, because several studies about their packing properties exist, both in the case of impenetrable, partially penetrable or fully impenetrable spheres.[30]

In the case of a very dilute suspension of spherical traps per unit volume with radius R, the trapping rate K_S (per unit trap) of small molecules is given by Smoluchowski's equation, which can be written as[1]

$$K_S = 4\pi D_{iff} R \quad (7)$$

where D_{iff} is the diffusion coefficient of a small molecule. We note that the notation used here is different from the one commonly adopted in the literature, where K_S is not the trapping rate per trap, as in (eq 7), but it is multiplied by the number concentration of traps, leading to a trapping rate per unit volume.

It is well-known that, as the concentration of traps increases, the trapping rate reaches values much higher than predicted by Smoluchowski's law (eq 7), as simulations have shown.[41] There are several theoretical studies that have set the goal of finding analytical expressions for the trap volume fraction dependence of the trapping rate. Nevertheless, most of these expression are only accurate for moderate volume fractions. One notable exceptions is the equation proposed by Richards, which predicts very accurately the concentration dependence of the trapping rate K for systems of fully penetrable spherical traps at an arbitrary nominal volume fraction ϕ:[37]

$$\gamma = \frac{K}{K_S} = \frac{1}{1 - \sqrt{3\phi}\exp\left(\frac{3\phi}{\pi}\right)\mathrm{erfc}\left(\sqrt{\frac{3\phi}{\pi}}\right)} \quad (8)$$

where $\mathrm{erfc}(x)$ is the complementary error function. It is worth noting that the nominal trap volume fraction ϕ in (eq 8) does not represent the volume fraction of space effectively occupied by the traps, but just the nominal trap volume fraction. It is well-known that the effective volume fraction ϕ_{eff} occupied by monodisperse overlapping spheres with nominal volume fraction ϕ is given by[30]

$$\phi_{eff} = 1 - \exp(-\phi) \quad (9)$$

The meaning of (eq 9) is that, as the nominal concentration of traps increases, the chance of overlap increases even more, leading to a very slow increase in the effective occupied volume fraction.

The aggregation of fractal clusters driven by diffusion bears many similarities with the trapping problem, but presents some notable differences. First of all, in a suspension undergoing diffusion-limited aggregation there is no difference between traps and diffusing species. Smoluchowski solved the problem by considering the relative motion of one particle with respect to another one, so that in (eq 7) the mutual diffusion coefficient

(i.e., the sum of both diffusion constants) and the collision radius (i.e., the sum of both radii)[1] appear. We will adopt the same scheme here, considering the relative motion of a cluster with respect the others. Second, clusters are not spheres, but can be represented as equivalent spheres with a properly defined radius. Additionally, clusters have a finite size, and their rate of diffusion limited aggregation needs to be connected to the trapping rate of finite size particles. Torquato considered the trapping rate of finite size Brownian particles, and concluded that the problem could be reduced to the case of point size particles diffusing in system of larger traps, with a size equal to the sum of the sizes of the trap and of the diffusing particle.[54] These larger traps have a core−shell morphology. Their core (corresponding to the original immobile trap) is impenetrable, while their shell (the diffusing particle contribution) is in fact penetrable. These assumptions are schematically depicted in Figure 1.

We will now develop a procedure to apply (eq 8) to compute a correction to the kinetics of aggregation of particles under diffusion-limited conditions at high volume fractions. Equation 8 is in principle only applicable to fully overlapping spherical traps, while the situation schematically depicted in Figure 1 refers to traps with only a penetrable shell. Torquato[54] showed that the trapping rate of different types of monodisperse spherical traps (impenetrable, partially penetrable and totally impenetrable spheres) collapse in a mastercurve, when plotted as a function of the effective occupied volume fraction and normalized by a suitable power of the total effective surface.[54] This means that Richards equation can be used to interpret all the available data on trapping rate, as long as the effective volume and the effective surface of the different configurations can be computed. In the case of fractal clusters, however, the situation is complex. A population of clusters undergoing diffusion-limited cluster aggregation becomes progressively more polydisperse with time, and a relationship between the nominal volume and the effective volume fraction or the effective surface for partially interpenetrating spheres exists only for the monodisperse case. Finally, the exponent values appearing in the power law mentioned by Torquato have only been reported for one value of core/shell ratio.[54] For all these reasons, we will only make use of the scaling with the effective volume fraction and will neglect the contribution of the specific surface.

The adopted procedure works as follows. The cluster occupied volume fraction ϕ_c is first calculated according to

$$\phi_c = \sum_{i=1}^{\infty} N_i \frac{4}{3}\pi R_i^3 \tag{10}$$

where N_i is the number of clusters with mass i per unit volume and R_i their suitably defined radius. We consider an aggregation event involving a cluster with mass k, and we convert it to the corresponding trapping event with a point-like cluster k as the diffusing species, with all other clusters as the traps. The relevant nominal volume fraction of the traps ϕ_n is given by

$$\phi_n = \sum_{i=1}^{\infty} N_i \frac{4}{3}\pi (R_i + R_k)^3 \tag{11}$$

where to the radius of the generic ith cluster the radius of the kth cluster is added. An average ratio between the trap core radius and its shell radius is defined as

$$\lambda = \left(\frac{\phi_c}{\phi_n}\right)^{1/3} \tag{12}$$

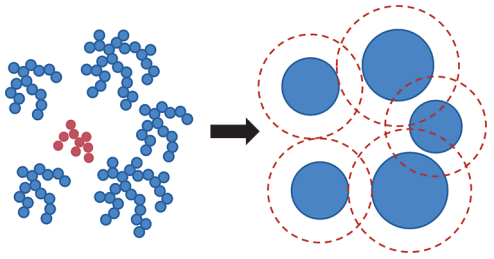

Figure 1. Schematics showing how the diffusion-limited aggregation of a specific fractal cluster (in red) with a group of other clusters (in blue, to the left) is reinterpreted within the trap theory as diffusion-limited reaction of a point-object within a group of spherical traps, each having an outer radius equal to the sum of the radii of the original and of the diffusing clusters, with an impenetrable core (blue) and penetrable shell (red).

As previously explained, the traps defined in this manner are of core−shell type, with impenetrable core, but penetrable shell. In order to compute the effective volume fraction occupied by the core−shell traps, with nominal volume fraction ϕ_n, we make use of the following equation reported by Torquato et al.:[30]

$$\phi_{\text{eff}} = 1 - (1 - \phi_n\lambda^3)\exp\left(-\frac{\phi_n(1-\lambda^3)}{(1-\phi_n\lambda^3)^3}\right) \exp\left(-\frac{\phi_n^2\lambda^3(\lambda-1)}{2(1-\phi_n\lambda^3)^3}[(7\lambda^2 + 7\lambda - 2) - 2\phi_n\lambda^3(7\lambda^2 - 5\lambda + 1) + \phi_n{}^2\lambda^6(5\lambda^2 - 7\lambda + 2)]\right) \tag{13}$$

In order to use eq 8, we need the nominal volume fraction of fully penetrable traps that has the same effective volume fraction of our core−shell traps. With the effectively occupied volume fraction ϕ_{eff}, we can use eq 9 to compute the nominal volume fraction ϕ of fully penetrable traps that have an effective occupied volume fraction ϕ_{eff}. ϕ is given by:

$$\phi = -\log(1 - \phi_{\text{eff}}) \tag{14}$$

Once ϕ is known, eq 8 can be used to compute the correction factor for the aggregation rate involving clusters with mass k.

To summarize, the correction factor for a cluster of mass k is given by eq 8, in which the volume fraction ϕ is computed using eqs 10−14. The correction factor estimated in this manner is cluster size dependent. It however important to pinpoint that the aggregation event between one cluster with mass i and another one with mass j, can be consider both as the diffusion of aggregate i toward aggregate j or viceversa. Similarly, it is arbitrary to assign the status of trap to one of the two clusters. This is a critical point, because the correction factor computed assuming that a large cluster is the diffusing one will be much larger than that of a smaller cluster. In this work, we decided to use for the aggregation even between clusters i and j an average correction factor weighed by the diffusion coefficients of the two clusters, in order to give a stronger contribution to the small and more mobile clusters. Explicitly, for an aggregation event involving two clusters, one with mass i and one with mass j:

$$f_{corr,ij} = \frac{\left(\frac{\gamma(i)}{R_{h,i}} + \frac{\gamma(j)}{R_{h,j}}\right)}{\frac{1}{R_{h,i}} + \frac{1}{R_{h,j}}} \tag{15}$$

dx.doi.org/10.1021/jp2097839 |J. Phys. Chem. B 2012, 116, 120–129

Here $\gamma(i)$ is the correction factor computed from eq 8 as described before i, and $R_{h,i}$ the hydrodynamic radius of a clusters with mass i. In eq 15 Stokes−Einstein equation was used, according to which the diffusion coefficient of a cluster is inversely proportional to its hydrodynamic radius.

The last important point to be discussed is the cluster characteristic size R_i to be used in eq 10 and eq 11. For primary particles, their radius has been used. For all the other clusters, instead, the sphere radius leads to excessive overestimation of the volume fraction, especially when considered that fractal clusters do not have a compact structure and are prone to a certain degree of interpenetration. However, very small clusters can interpenetrate less than large clusters. In account of this observation, we have found that small cluster (doublets, trimers, tetramers) deserve a special treatment, and their effective radii are respectively 25%, 15%, 5%, larger than their radii of gyration. On the other hand, for clusters with more then five particles a characteristic size equal to 95% of their radius of gyration is used.

PBES CALCULATIONS

The calculations of nanoparticles aggregation under diffusion-limited conditions have been performed by numerically solving population balance equations. The aggregation of particles and clusters thereof has been assumed to be an irreversible process, which can be modeled as a second order kinetic process. In this case PBEs are written as follows:[16]

$$\frac{dN_k}{dt} = \frac{1}{2}\sum_{i,j=1}^{i+j=k} K_{ij}N_iN_j - N_k\sum_{i=1}^{\infty} K_{ik}N_i \qquad (16)$$

where N_i is the number concentration of clusters with mass i (i.e., made of i particles), and K_{ij} is the kernel determining the rate of aggregation between two clusters, one with mass i and the other with mass j.

The aggregation kernel used in the simulations consists of a corrected form of the conventional diffusion-limited aggregation kernel, which has the following form:[1]

$$K_{ij} = f_{corr,ij}\frac{2kT}{3\eta W}(i^{1/d_f} + j^{1/d_f})(i^{-1/d_f} + j^{-1/d_f}) \qquad (17)$$

W is the primary particles Fuchs stability ratio, η is the viscosity of water, k the Boltzmann constant, T the temperature, d_f is the cluster fractal dimension, and $f_{corr,ij}$ is the correction factor accounting for the volume fraction dependence of the aggregation process, and is given by eq 15.

The Fuchs stability ratio W in (eq 17) is computed from its definition:[1]

$$W = 2\int_2^{\infty} \frac{\exp\left(\frac{U_{VdW}}{kT}\right)}{x^2}\,dx \qquad (18)$$

where x is the dimensionless distance between two particles centers normalized by the particle radius R_p and U_{VdW} is the van der Waals interaction energy between two primary particles, which is given by (eq 3). Note that in the definition of the Fuchs stability ratio (eq 18), no correction for hydrodynamic interaction between the particles has been included, because in BD simulations hydrodynamic interactions have also been neglected.

In order to relate a cluster mass with its size, the equations outlined in a previous work have been utilized.[55,56] These account in an accurate manner for the structure of small clusters, with a mass up to four particles, and treat all bigger clusters as fractals. Even though the correlations and parameter values were developed for classical DLCA and RLCA clusters, these where extrapolated also to clusters with higher fractal dimensions, such as those obtained at higher volume fractions.

The numerical solution of the population balance equations has been performed by means of the Kumar−Ramkrishna (KR) method, as described elsewhere.[4,57] With the KR method, a wide rage of cluster mass values is divided into intervals using a logarithmic spacing. The PBEs are solved for all the mass values corresponding to the boundaries of each interval, usually called pivots. Each time an aggregation event leads to the production of a cluster with mass falling inside one interval, the cluster is split between the two boundaries of the interval. The splitting factors are selected in order to preserve the first two moments of the original distribution. This procedure guaranties a high efficiency of the code, which allows one to simulate the evolution of a very broad cluster mass distribution. However, the presence of the volume fraction dependent correction factors renders the numerical solution of the KR equations more challenging as they become significantly stiffer. For this reason, the maximum value of the correction factor $f_{corr,ij}$ has been bounded to 100, in order to limit the stiffness of the equations.

RESULTS AND DISCUSSION

In this work, we developed a new kernel capable of accurately predicting the kinetics of diffusion-limited aggregation processes at high volume fractions up to the gel point. Since performing experiments of diffusion limited aggregation kinetics at high concentrations is extremely challenging because of the very short characteristic times of aggregation and gelation for common colloidal suspensions, we used BD simulations to monitor the kinetics of the process and to have a reliable comparison for PBEs calculations.

The BD algorithm used in this works differs somehow from those reported in the literature because it has been specifically designed to account for irreversible aggregation. In order to achieve this, it features some characteristics of conventional Monte Carlo cluster−cluster algorithms. First of all, bonds between particles are irreversible. Since clusters are moved as rigid bodies, it is necessary to accurately account for their mobilities and diffusion tensors.[50] The theory developed by Garcia de la Torre et al.[51−53] has been used to compute the hydrodynamic properties of clusters. In this manner, even though hydrodynamic interactions among clusters are neglected, those among particles belonging to the same cluster have been accounted for, and the mobility tensors of clusters are consistent with their fractal morphology. Furthermore, the proposed algorithm takes into account not only translational but also rotational motion of clusters, thus rendering the cluster dynamics and aggregation kinetics more realistic.

In order to perform PBEs calculations, the cluster fractal dimension has to be known. BD simulation results indicate that as the particle volume fraction increases, denser clusters are formed. The fractal dimension values d_f determined from BD simulations are reported in table Table 1. These values, which are in good agreement with those reported by Gonzalez et al.,[10,11,58] and obtained using Monte Carlo simulations, range from 1.85 for $\phi_p = 0.01$ until 2.35 for $\phi_p = 0.3$.

The corrected kernel used in this work, given by (eq 17), was obtained as explained in detail in eq 6. We started from concepts borrowed from trapping theory, in which the effect of trap

Table 1. Cluster Fractal Dimension Values for All the Particle Volume Fractions Investigated in This Work, Obtained from BD Simulations and Utilized in PBEs Calculations

ϕ_p	0.01	0.05	0.1	0.15	0.2	0.25	0.3
d_f	1.85	1.93	2	2.1	2.2	2.3	2.35

volume fraction on the rate of diffusion-limited reaction has been systematically investigated, and we adapted them to the aggregation of fractal clusters. The assumptions that fractal clusters can be considered as partially interpenetrable spheres is commonly adopted when dealing with fractal clusters. The correction to the rate of aggregation accounting for high concentrations is obtained by using the Richards equation, eq 8, which was obtained in the case of point-like objects diffusing toward immobile spherical fully penetrable traps.[35] In order to apply it to fractal clusters, an event involving one diffusing cluster toward all other clusters was first considered. An effective volume fraction occupied by all other clusters and including the size of the diffusing cluster was defined by eq 13, in order to translate the aggregation event of finite size object into an equivalent trapping event of a point-like object. Then (eq 8) was used with a nominal volume fraction of fully penetrable traps that leads to the same effective volume fraction as estimated from eq 13. The correction estimated in this way refers to a given cluster diffusing and reacting with any other clusters. In order to provide a correction for a binary event involving two clusters, with masses i and j, we decided to use a average of the two corrections weighted by the diffusion coefficient of each cluster, as expressed by eq 17. The implementation of the proposed correction into a PBEs kinetic scheme leads to an overall aggregation rate increase both as the primary particle volume fraction increases, and as the aggregation proceeds, because of the progressively higher occupied volume fraction by the fractal clusters.

We now turn our attention to the kinetics of aggregation. We performed a comparison between the results from BD simulations and the predictions from PBE calculation, using the new kernel illustrated in the previous section, i.e., eq 17. We analyzed in detail the time evolution of the total number of clusters, of the first two moments of the cluster mass distribution (CMD), of the clusters occupied volume fraction. The n^{th} moment M_n of the CMD has been defined as

$$M_n = \frac{\sum_{i=1}^{\infty} N_i i^n}{\sum_{i=1}^{\infty} N_i i^{n-1}} \tag{19}$$

and the occupied volume fraction by the clusters ϕ_o has been defined as

$$\phi_o = \sum_{i=1}^{\infty} N_i \frac{4}{3}\pi R_i^3 \tag{20}$$

where R_i is the outer radius for primary particles, and the radius of gyration for all the other clusters.

Figure 2 shows the time evolution of the total number of clusters in the systems $N_t = \Sigma_{i=1}^{\infty} N_i$, normalized by the initial number of primary particles per unit volume N_0, up to the gel point. The time has been normalized by Smoluchowski's time constant $\tau = (3\eta)/(8kTN_0)$. The normalization of the time provided by Smoluchowski's time constant should account for all

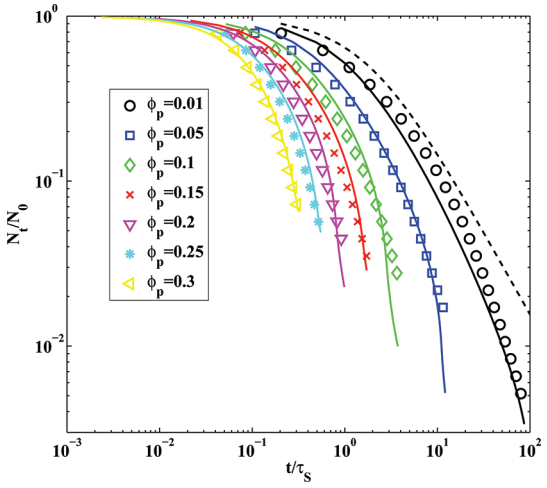

Figure 2. Time evolution of dimensionless number of clusters from BD simulations for seven different particle volume fractions, as indicated in the legend. The continuous lines are the predictions from PBE calculations using the corrected kernel, eq 17. The dashed line is the prediction from PBE calculations using the noncorrected Smoluchowski's kernel.

the differences in aggregation kinetics with particle volume fraction, if the system behaved as predicted by the classical Smoluchowski's theory, because PBEs (eq 16) can be written in volume fraction independent dimensionless form when this normalized time constant is used.[4] What can be immediately captured from Figure 2 is that BD simulations predict instead a strong dependence of the time evolution of the cluster number on the initial particle volume fraction. As the particle volume fraction increases, a substantial increase in the rate at which the total number of clusters decreases is observed. Additionally, for volume fractions higher than 15%, the curves show and inflection point, characterized by very rapid cluster consumption rate after a given time. The point of inflection coincides with the gel point. The dashed line in the same figure shows the prediction obtained using classical Smoluchowski's kernel, i.e., (eq 17) with the correction factor $f_{corr,ij}$ = 1. The calculation shown was made only for a fractal dimension equal to 1.85, corresponding to the value obtained from BD simulations for low particle volume fraction. The curves for higher fractal dimension values have not been reported in Figure 2 as thy are identical, when plotted as a function of dimensionless time. It is clearly observed that PBE simulations performed using the ideal DLCA kernel slightly underpredict the cluster consumption rate observed for a volume fraction of 1%, but substantially underpredict the rate of cluster consumption at high volume fractions. The difference between PBE calculations and BD simulations results progressively increase up to a factor of at least 20 with the particle volume fraction. Clearly, classical Smoluchowsky's theory is unable to properly account for the high volume fraction aggregation behavior.

Figure 2 also shows the predictions of PBE calculations using kernel eq 17 with the correction given by eq 15. One can clearly observe that the corrected version of the kernel, accounting for a volume fraction dependence of the aggregation rate, is cable of reproducing very accurately the BD data until the gel point, for all the volume fractions considered. The model is also capable of predicting the presence of a gel point, as seen as an inflection point in the curve. Differently from the BD results, however, the model predicts an inflection point for all values of the volume

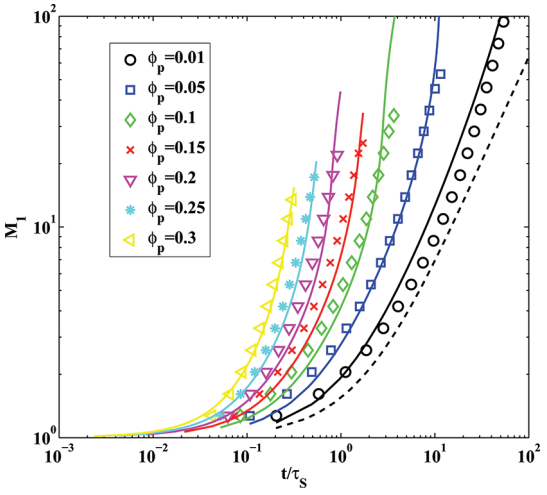

Figure 3. Time evolution of the first moment of the CMD from BD simulations for seven different particle volume fractions, as indicated in the legend. The continuous lines are the predictions from PBE calculations using the corrected kernel, eq 17. The dashed line is the prediction from PBE calculations using the noncorrected Smoluchowski's kernel.

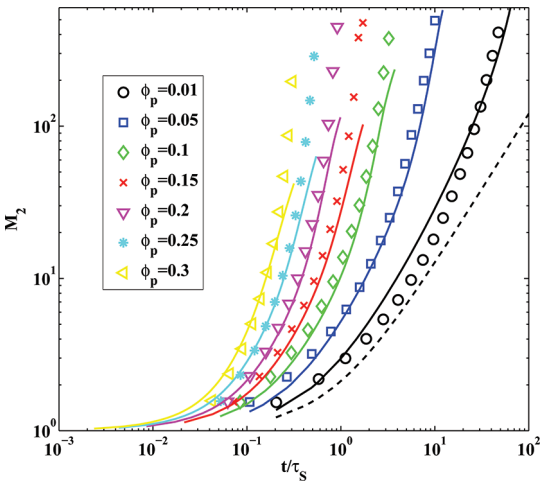

Figure 4. Time evolution of the second moment of the CMD from BD simulations for seven different particle volume fractions, as indicated in the legend. The continuous lines are the predictions from PBE calculations using the corrected kernel, eq 17. The dashed line is the prediction from PBE calculations using the noncorrected Smoluchowski's kernel.

fractions. The PBE simulations cannot simulate accurately the time evolution of the system after gelation (data not shown), since the formation of gel phase is not explicitly considered in the PBE model.

We now draw our attention to the first two moments of the CMD, i.e., the number-average and weight-average mass of the CMD, respectively. The comparisons are shown in Figure 3 and Figure 4 for the first and second moment, respectively, once more up to the gel point. In both figures it can be observed that the corrected kernel is capable of representing very accurately the time evolution of the first moment of the CMD, including the final acceleration in the growth rate. As a comparison, the prediction from classical Smoluchowski's theory is also shown

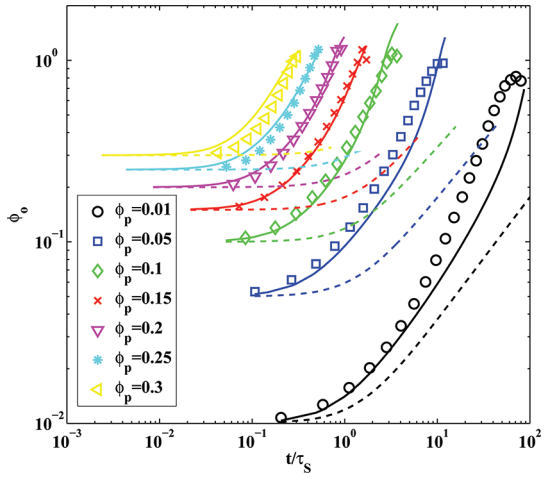

Figure 5. Time evolution of the clusters occupied volume fraction from BD simulations for seven different particle volume fractions, as indicated in the legend. The continuous lines are the predictions from PBE calculations using the corrected kernel, eq 17. The dashed lines are the predictions from PBE calculations using the noncorrected Smoluchowski's kernel.

(dashed line), which is independent of the cluster fractal dimension and clearly indicates how classical Smoluchowski's theory already starts underpredicting the BD simulation results at a volume fraction of 1%, in particular at later stages of the aggregation. The comparison of the second moment of the CMD shows again a satisfactory agreement, with some deviations observed close to the gel point for the highest volume fractions. This indicates that most probably the PBE simulations are underestimating the concentration of large clusters, the role of which is more important in the second moment than in the first one. In all cases, the deviations of classical Smoluchowski's theory from BD simulations results at the highest particles volume fraction value can be quantified by almost a factor of 20. However, this is only the deviation at the initial stages of the aggregation, because, as the aggregation proceeds, the crowding effect becomes even stronger, as one can appreciated by comparing the different slopes of the PBE predictions obtained using the corrected kernel with the uncorrected one.

Figure 5 shows instead the clusters occupied volume fraction evolution with dimensionless time. The comparison between PBE calculations with the corrected kernel and BD simulation results is very satisfactory for all volume fractions until the gel point. It is important to point out here that the gel point for most of the cases considered occurs at an occupied volume fraction ϕ_o very close to unity, as expected from simple scaling arguments. Classical Smoluchowski's theory, on the other hand, substantially underestimates the growth of the volume fraction with time, leading only to satisfactory results for the initial growth of the lowest volume fraction case considered, i.e., $\phi_p = 0.01$. By looking at the time required to have $\phi_o = 1$, we could make a prediction of the gel point, and comparing to BD simulations. The results are shown in Figure 6, together with the predictions form the uncorrected DLCA kernel. It is possible to observe that the corrected kernel allows one to make very accurate predictions of gel time, while the uncorrected kernel underestimates the gel point by 20 to 50 times.

dx.doi.org/10.1021/jp2097839 |*J. Phys. Chem. B* 2012, 116, 120–129

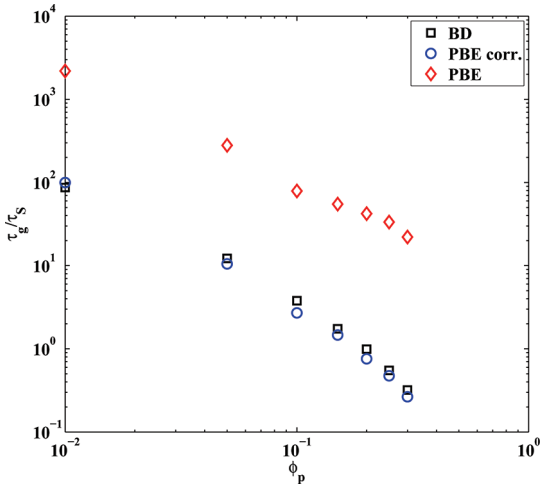

Figure 6. Gel time as a function of the particle volume fraction ϕ_p from BD simulations, compared to the predictions from PBE calculations using the corrected kernel, (eq 17) and the traditional noncorrected Smoluchowski's kernel.

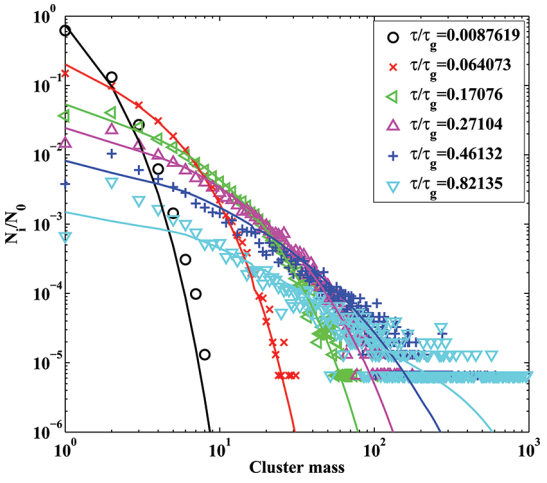

Figure 7. CMDs from BD simulations at ϕ_p = 0.05 for the dimensionless time values indicated in the legend. The continuous lines are the predictions from PBE calculations using the corrected kernel, eq 17.

We conclude our comparison by showing a few CMDs, at selected times, from both BD simulations and PBE calculations using the corrected kernel for three volume fractions: 5%, 20%. and 30%. The comparison is shown in Figures 7, 8, and 9 for the dimensionless times reported in the legends. These dimensionless times were normalized by using the gel point. It can be observed that, within the errors and uncertainties from BD simulations, the agreement is good, especially for intermediate volume fractions. This indicates that the corrected kernel introduced in this work is able to accurately follow the kinetics of the aggregation process at high volume fractions up to the gel point. One can however observe that, as the system approaches the gel point, PBE calculations tend to slightly underestimate the concentration of the largest clusters, forming a tail in the CMD. The discrepancies observed in the predictions of the second moments in the CMD are most probably related to the importance of this tail in the CMD, as observed in Figures 7, 8, and 9 at

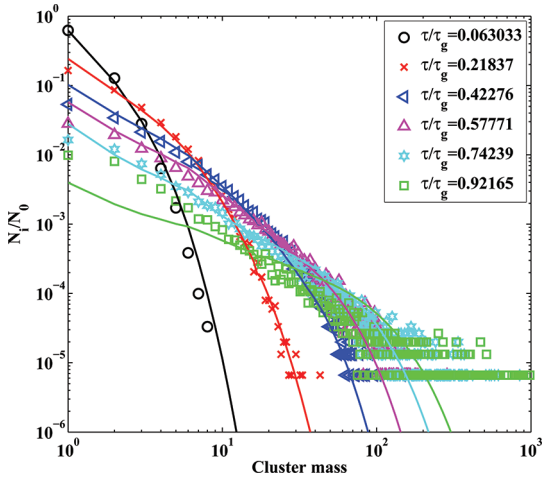

Figure 8. CMDs from BD simulations at ϕ_p = 0.2 for the dimensionless time values indicated in the legend. The continuous lines are the predictions from PBE calculations using the corrected kernel, eq 17.

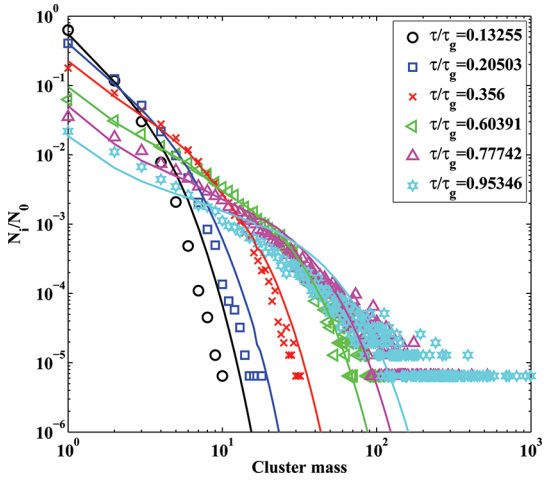

Figure 9. CMDs from BD simulations at ϕ_p = 0.3 for the dimensionless time values indicated in the legend. The continuous lines are the predictions from PBE calculations using the corrected kernel, eq 17.

longer times. This effect is especially visible in Figure 9, corresponding to the highest particle volume fraction.

CONCLUSIONS

In this work, we have proposed an extension of Smoluchowski's diffusion-limited aggregation rate kernel capable of accounting for high concentration effects, using concepts developed within the framework of trapping theory. The expression of the aggregation rate uses an extrapolation of Richards equation, proposed to compute the rate of diffusion limited-reaction for point-like molecules reacting with a set of fully penetrable spherical traps, and extends it to fractal clusters. Under diffusion-limited aggregation conditions, all clusters can react with each other, and there is no distinction between traps and reacting molecules. Fractal clusters are treated as partially penetrable spheres, and a correction is introduced to account for the finite size of diffusing clusters. The rate expression developed in this manner predicts a progressive increase of the rate of aggregation not only as a

dx.doi.org/10.1021/jp2097839 |J. Phys. Chem. B 2012, 116, 120–129

function of the initial particle volume fraction, but also as a function of time, because the fractal clusters increase their occupied volume fraction as the aggregation proceeds. The aggregation rate is implemented in a population balance equations scheme, in order to make calculations of the full evolution of the aggregation rate constant.

In order to test the predictions of the kernel, Brownian dynamic simulations of particle aggregation in a broad range of particle volume fractions have been performed, using an in-house developed code. In these simulations particles are assumed to experience only van der Waals interactions, and all bonds formed as a result of aggregation are assumed to be irreversible. The movement of clusters made of more than one particle is modeled according to rigid body motion equations. BD simulations have been used to monitor the time evolution of the full cluster mass distribution, the time required to reach the gel point, and the cluster fractal dimension values used also in PBEs simulations.

The newly developed kernel allows one to make accurate predictions of the time evolution of the cluster mass distribution, of the first two moments of the CMD, of the occupied volume fraction and of the gel point as a function of particle volume fraction. The gel point in the PBEs model is identified as the point where the effective volume fraction reaches unity. In comparison, classical Smoluchowski's theory substantially underpredicts the rate of aggregation, and the time evolution of all moments of the CMDs, included the gel point, especially at high particle volume fractions.

In synthesis, the proposed kernel is the first physically sound model that allows one to extend the predictions of Smoluchowski's equation to aggregation under high concentrations. It is expected that the approach used in this work can be extended to more complex situations, such as aggregation under reaction-limited conditions.

AUTHOR INFORMATION

Corresponding Author

*E-mail: marco.lattuada@chem.ethz.ch.

ACKNOWLEDGMENT

This work was financially supported by the Swiss National Science Foundation (Grants No. 200020-126487/1 and 200020-132843). Many useful discussions with Prof. Massimo Morbidelli and Dr. Hua Wu are gratefully acknowledged.

REFERENCES

(1) Russel, D. A. S. W. R., William, B.; Saville *Colloidal Dispersions*; Cambridge University Press: London, 1989.
(2) Hunter, R. J. *Introduction to Modern Colloid Science*; Oxford University Press: New York, 2001.
(3) Berg, J. C. *An Introduction to Interfaces and Colloids: The Bridge to Nanoscience*; World Scientific: Singapore, 2010.
(4) Lattuada, M.; Wu, H.; Sandkuhler, P.; Sefcik, J.; Morbidelli, M. *Chem. Eng. Sci.* **2004**, *59*, 1783–1798.
(5) Lin, M. Y.; Lindsay, H. M.; Weitz, D. A.; Ball, R. C.; Klein, R.; Meakin, P. *Nature* **1989**, *339*, 360–362.
(6) Lin, M. Y.; Lindsay, H. M.; Weitz, D. A.; Ball, R. C.; Klein, R.; Meakin, P. *Phys. Rev. A* **1990**, *41*, 2005–2020.
(7) Lin, M. Y.; Lindsay, H. M.; Weitz, D. A.; Klein, R.; Ball, R. C.; Meakin, P. *J. Phys.: Condens. Matter* **1990**, *2*, 3093–3113.
(8) Dickinson, E. *J. Chem. Soc., Faraday Trans.* **1997**, *93*, 111–114.
(9) Dickinson, E.; Allison, S. A.; McCammon, J. A. *J. Chem. Soc., Faraday Trans. 2* **1985**, *81*, 591–601.
(10) Gonzalez, A. E.; Martinez-Lopez, F.; Moncho-Jorda, A.; Hidalgo-Alvarez, R. *Phys. A: Stat. Mech. Appl.* **2002**, *314*, 235–245.
(11) Gonzalez, A. E.; Martinez-Lopez, F.; Moncho-Jorda, A.; Hidalgo-Alvarez, R. *J. Colloid Interface Sci.* **2002**, *246*, 227–234.
(12) Adachi, Y. *Adv. Colloid Interface Sci.* **1995**, *56*, 1–31.
(13) Meakin, P. *Phys. Rev. Lett.* **1983**, *51*, 1119–1122.
(14) Meakin, P. *Adv. Colloid Interface Sci.* **1988**, *28*, 249–331.
(15) Meakin, P. *Annu. Rev. Phys. Chem.* **1988**, *39*, 237–267.
(16) Ramkrishna, D. *Population Balances: Theory and Applications to Particulate Systems in Engineering*; Academic Press: London, 2000.
(17) Leyvraz, F. *Phys. Rep., Rev. Sect. Phys. Lett.* **2003**, *383*, 95–212.
(18) von Smoluchowski, M. *Z. Phys. Chem., Stochiom. Verwandtschaftsl.* **1917**, *92*, 129–168.
(19) Lichtenfeld, H.; Stechemesser, H.; Mohwald, H. *J. Colloid Interface Sci.* **2004**, *276*, 97–105.
(20) Holthoff, H.; Egelhaaf, S. U.; Borkovec, M.; Schurtenberger, P.; Sticher, H. *Langmuir* **1996**, *12*, 5541–5549.
(21) Fukasawa, T.; Adachi, Y. *J. Colloid Interface Sci.* **2006**, *304*, 115–118.
(22) Heine, M. C.; Pratsinis, S. E. *Langmuir* **2007**, *23*, 9882–9890.
(23) Buesser, B.; Heine, M. C.; Pratsinis, S. E. *J. Aerosol Sci.* **2009**, *40*, 89–100.
(24) Hutter, M. *Phys. Chem. Chem. Phys.* **1999**, *1*, 4429–4436.
(25) Kusaka, Y.; Fukasawa, T.; Adachi, Y. *J. Colloid Interface Sci.* **2011**, *363*, 34–41.
(26) Sciortino, F.; Belloni, A.; Tartaglia, P. *Phys. Rev. E* **1995**, *52*, 4068–4079.
(27) Sciortino, F.; Tartaglia, P. *Phys. Rev. Lett.* **1995**, *74*, 282–285.
(28) Carpineti, M.; Giglio, M. *Phys. Rev. Lett.* **1992**, *68*, 3327–3330.
(29) Bremer, L. G. B.; Bijsterbosch, B. H.; Walstra, P.; Vanvliet, T. *Adv. Colloid Interface Sci.* **1993**, *46*, 117–128.
(30) Torquato, S. *Random Heterogeneous Materials*; Springer: New York, 2001.
(31) Cukier, R. I.; Freed, K. F. *J. Chem. Phys.* **1983**, *78*, 2573–2578.
(32) Felderhof, B. U.; Deutch, J. M. *J. Chem. Phys.* **1976**, *64*, 4551–4558.
(33) Muthukumar, M. *J. Chem. Phys.* **1982**, *76*, 2667–2671.
(34) Muthukumar, M.; Cukier, R. I. *J. Stat. Phys.* **1981**, *26*, 453–469.
(35) Richards, P. M. *J. Chem. Phys.* **1986**, *85*, 3520–3529.
(36) Richards, P. M. *Phys. Rev. Lett.* **1986**, *56*, 1838–1841.
(37) Richards, P. M. *Phys. Rev. B* **1987**, *35*, 248–256.
(38) Lee, S. B.; Kim, I. C.; Miller, C. A.; Torquato, S. *Phys. Rev. B* **1989**, *39*, 11833–11839.
(39) Miller, C. A.; Kim, I. C.; Torquato, S. *J. Chem. Phys.* **1991**, *94*, 5592–5598.
(40) Miller, C. A.; Torquato, S. *Phys. Rev. B* **1989**, *40*, 7101–7108.
(41) Torquato, S. *J. Stat. Phys.* **1991**, *65*, 1173–1206.
(42) Szabo, A. *J. Phys. Chem.* **1989**, *93*, 6929–6939.
(43) Mattern, K.; Felderhof, B. U. *Physica A* **1987**, *143*, 1–20.
(44) Gosele, U. *J. Nucl. Mater.* **1978**, *78*, 83–95.
(45) Fixman, M. *J. Chem. Phys.* **1984**, *81*, 3666–3677.
(46) Berezhkovskii, A. M.; Makhnovskii, Y. A.; Suris, R. A. *J. Stat. Phys.* **1991**, *65*, 1025–1041.
(47) Allen, M. P.; Tildeslay, D. *Computer Simulation of Liquids*; Oxford University Press: New York, 1989.
(48) Park, H.; Kim, S.; Chang, H. S. *J. Aerosol Sci.* **2001**, *32*, 1369–1388.
(49) Puertas, A. M.; Maroto, J. A.; Barbero, A. F.; de las Nieves, F. J. *Phys. Rev. E* **1999**, *59*, 1943–1947.
(50) Whittle, M.; Dickinson, E. *Mol. Phys.* **1997**, *90*, 739–757.
(51) Delatorre, J. G.; Bloomfield, V. A. *Q. Rev. Biophys.* **1981**, *14*, 81–139.

(52) Carrasco, B.; de la Torre, J. G. *Biophys. J.* **1999**, *76*, 3044–3057.
(53) Delatorre, J. G.; Martinez, M. C. L.; Molina, J. J. G. *Macromolecules* **1987**, *20*, 661–666.
(54) Torquato, S. *J. Chem. Phys.* **1991**, *95*, 2838–2841.
(55) Lattuada, M.; Wu, H.; Morbidelli, M. *J. Colloid Interface Sci.* **2003**, *268*, 106–120.
(56) Lattuada, M.; Wu, H.; Morbidelli, M. *J. Colloid Interface Sci.* **2003**, *268*, 96–105.
(57) Kumar, S.; Ramkrishna, D. *Chem. Eng. Sci.* **1996**, *51*, 1311–1332.
(58) Lachhab, M.; Gonzalez, A. E.; Blaisten Barojas, E. *Phys. Rev. E* **1996**, *54*, 5456–5462.